

THE OFFICIAL MAGAZINE OF THE OCEANOGRAPHY SOCIETY

Oceanography

CITATION

Tréhu, A.M., W.S.D. Wilcock, R. Hilmo, P. Bodin, J. Connolly, E.C. Roland, and J. Braunmiller. 2018. The role of the Ocean Observatories Initiative in monitoring the offshore earthquake activity of the Cascadia subduction zone. *Oceanography* 31(1):104–113, <https://doi.org/10.5670/oceanog.2018.116>.

DOI

<https://doi.org/10.5670/oceanog.2018.116>

COPYRIGHT

This article has been published in *Oceanography*, Volume 31, Number 1, a quarterly journal of The Oceanography Society. Copyright 2018 by The Oceanography Society. All rights reserved.

USAGE

Permission is granted to copy this article for use in teaching and research. Republication, systematic reproduction, or collective redistribution of any portion of this article by photocopy machine, reposting, or other means is permitted only with the approval of The Oceanography Society. Send all correspondence to: info@tos.org or The Oceanography Society, PO Box 1931, Rockville, MD 20849-1931, USA.

The Role of the Ocean Observatories Initiative in Monitoring the Offshore Earthquake Activity of the Cascadia Subduction Zone

By Anne M. Tréhu, William S.D. Wilcock, Rose Hilmo, Paul Bodin,
Jon Connolly, Emily C. Roland, and Jochen Braunmiller



Photo taken aboard R/V *Oceanus*
during cruise OC1205A, May 2012.
Photo credit: Daniel Zietlow

ABSTRACT. Geological and historical data indicate that the Cascadia subduction zone last ruptured in a major earthquake in 1700. The timing of the next event is currently impossible to predict, but recent studies of several large subduction zone earthquakes provide tantalizing hints of precursory activity. The seismometers at the Ocean Observatories Initiative (OOI) Slope Base and Southern Hydrate Ridge nodes are well placed to provide new insights into interplate coupling because they are located over a segment of the subduction zone that is nominally locked but that has been relatively active for more than a decade. Since their installation in 2014, 18 earthquakes with magnitudes up to 3.8 have been located by the Pacific Northwest Seismic Network between 44°N and 45°N in the region of the plate boundary thought to be accumulating strain. The OOI seismometers have also detected events that were not reported by the onshore seismic network. Noting that OOI data are available in real time, which is a necessary criterion for routine earthquake monitoring, and that the OOI seismometers generally have lower noise levels than campaign-style ocean bottom seismometers, there would be significant benefit to adding seismometers to existing nodes that are not yet instrumented with seismometers.

INTRODUCTION

The largest and some of the most damaging earthquakes in history have occurred in subduction zones, where one plate plunges beneath another plate. At the Cascadia subduction zone (Figure 1), which extends from northern California to Vancouver Island, the Juan de Fuca Plate is being subducted beneath the North American Plate. In several respects, Cascadia is an end member in the global spectrum of subduction zones (Wang and Tréhu, 2016). Because of the young age of the subducting plate (<15 million years), a relatively slow convergence rate (3–4 cm yr⁻¹), and abundant sediment supply that blankets subducting oceanic crust, the Cascadia plate boundary fault is hotter than most subduction megathrusts. It is also unusually free of recent earthquake activity (Figure 1).

Despite the low level of current earthquake activity, there is evidence for large (magnitude >8) historic and prehistoric earthquakes on the Cascadia megathrust. Tsunami records in Japan, coastal subsidence, and oral histories indicate there was a magnitude 8.7–9.2 earthquake at the Cascadia subduction zone on January 29, 1700 (Atwater et al., 2015). Onshore and offshore paleoseismic data indicate the occurrence of 20 large earthquakes in the past 10,000 years, with inter-event times ranging from 200 years to 1,200 years (Goldfinger et al., 2012).

The paucity of recent earthquakes can mean that the two plates are slipping past each other without generating earthquakes or that they are firmly locked together, storing elastic strain that will be released in a future large earthquake, or some combination thereof. Thermal models (e.g., Hyndman and Wang, 1993;

Cozzens and Spinelli, 2012) have been used to predict the boundary between the seismogenic zone, where the plates are cold and may be locked (temperature <350°–450°C), and a deeper zone of “episodic tremor and slip” (ETS), characterized by slow slip observed in GPS data accompanied by seismic tremor (Rogers and Dragert, 2003). Figure 1 shows the position of the 450°C isotherm (short dashed line) and the updip position of ETS (short/long dashed line), which are approximately coincident and may indicate the downdip limit of seismogenic slip in major subduction zone earthquakes (Hyndman, 2013; Wang and Tréhu, 2016). Note that the Cascadia seismogenic zone lies almost entirely offshore.

Global plate models (e.g., DeMets et al., 2010) predict that ~8 m of slip perpendicular to the margin has accumulated off central Oregon since 1700. This slip deficit is large enough to generate a magnitude 8 or larger earthquake if it is released through sudden slip on the shallow (offshore) plate

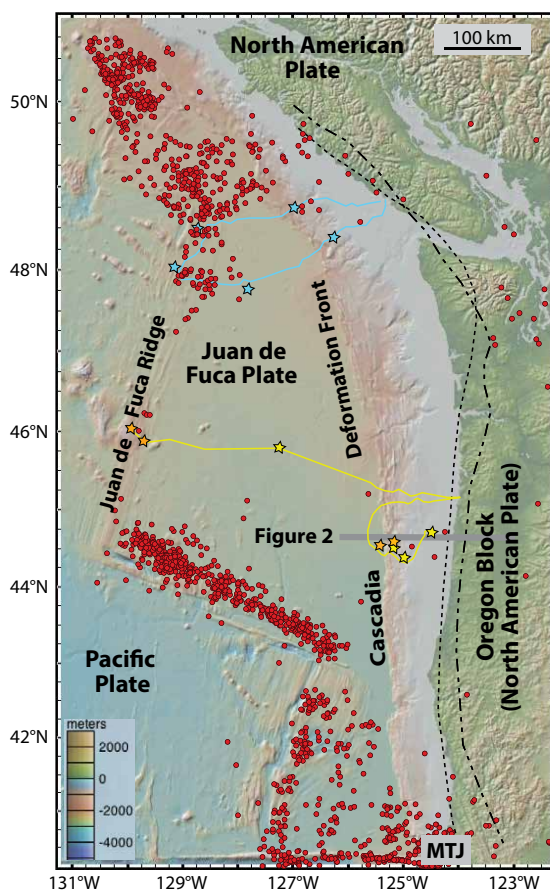


FIGURE 1. Topographic map of the US Pacific Northwest using data from the Global Multi-Resolution Topographic database accessed via GeoMapApp (<http://www.geomapapp.org>). Earthquakes with magnitudes ≥ 4 from January 1989 through August 2017 in the Advanced National Seismic System (ANSS) Comprehensive Earthquake Catalog (<https://earthquake.usgs.gov/data/comcat>) are shown as red dots. The surface trace of the boundary between the Juan de Fuca and North American Plates coincides with the abrupt deformation front seen in the topography of the continental margin. The short dashed line is the 450°C contour, the short/long dashed line is the updip limit of tremor from 2005 to 2011, and the dark gray line is the location of the cross section in Figure 2. The yellow line shows the OOI cable route. Stars show nodes with (orange) and without (yellow) seismometers. Blue lines and stars show the NEPTUNE cabled observatory.

boundary (Tréhu, 2016). To evaluate the seismic hazard in Cascadia, it is important to understand how much of the potential slip is being stored, to be released in a future great subduction zone earthquake, and how much is being accommodated through aseismic slip and small earthquakes on the plate boundary or by internal deformation of the Juan de Fuca and North American Plates. Developing this understanding requires knowledge of where offshore earthquakes occur. Moreover, recent results from subduction zone earthquakes elsewhere show that at least some earthquakes are preceded by distinctive foreshock activity and/or slow slip within the seismogenic zone (e.g., Bouchon et al., 2013; Ito et al., 2013; Burgmann, 2014). As these precursory patterns become better documented and modeled, their value for earthquake forecasting should increase.

The objective of this paper is to determine the value of seismometers located at the Ocean Observatories Initiative (OOI) Slope Base (SB) and Southern Hydrate Ridge (SHR) nodes to the detection and location of earthquakes on the Cascadia margin. Through coincidence, the OOI SB-SHR network is located near an anomalous segment of the margin that

has been the site of persistent seismicity in the magnitude 2–5 range since at least 1989 (Tréhu et al., 2015). Between November 4, 2014, when data from the OOI SB-SHR network became available through the IRIS Data Management Center, and September 30, 2017, 18 earthquakes with magnitudes up to 3.8 were reported by the Pacific Northwest Seismic Network (PNSN) between 44°N and 45°N and 125.5°W and 124°W. In addition, from November 2014 to October 2015, the Cascadia Initiative ocean bottom seismometer (OBS) network (Toomey et al., 2014) operated simultaneously with the OOI SB-SHR network, providing the opportunity to compare signal-to-noise ratios and evaluate the impact of potential expansion of the OOI seismic network.

BACKGROUND

The Challenge of Recording Seismic Waves Offshore

Earthquakes radiate seismic energy across a range of frequencies, with larger earthquakes generating relatively more low-frequency energy. The seismic waves are recorded using sensors that typically record three orthogonal components of ground motion. Development of portable broadband sensors in the 1980s greatly

expanded the ability of onshore seismologists to record seismic waves at many locations and across a wide frequency band, improving their ability to resolve Earth structure and earthquake source processes. Expansion of this capability to the ocean has been difficult because of the exceptionally low shear strength of marine sediments and the high noise levels generated by nonlinear interactions and direct effects of ocean waves (e.g., Webb, 1998). Moreover, conventional OBS designs include power, buoyancy, timing control, and data recording in a single package. The resulting bulky package is more susceptible to narrow-band frequency resonances and is more attractive to seafloor fauna, which disturb the instrument, generating signals, termed “bio-bumps,” that can obscure local earthquakes. Many of these noise sources are potentially mitigated by OOI sensors because on the Cascadia margin they are buried in seafloor sediments and separated from the power and recording hardware.

The Challenge of Locating Offshore Earthquakes

An earthquake is located by determining the arrival times of the seismic waves it generates on a network of seismometers. Accurate determination of source latitude and longitude requires a good azimuthal distribution of seismic stations around an earthquake and knowledge of the velocity with which seismic waves travel through the rocks from the source to the receiver. Both requirements are problematic when only onshore data are available to locate small earthquakes on the shallow part of subduction zone plate boundaries, which are generally offshore. Moreover, the crustal thickness and velocity structure change dramatically across the continent-ocean margin (Figure 2), which is generally not taken into account for routine earthquake monitoring.

To interpret the tectonic implications of earthquakes, it is important to determine their depth. A general rule of thumb for resolving depth from observed travel

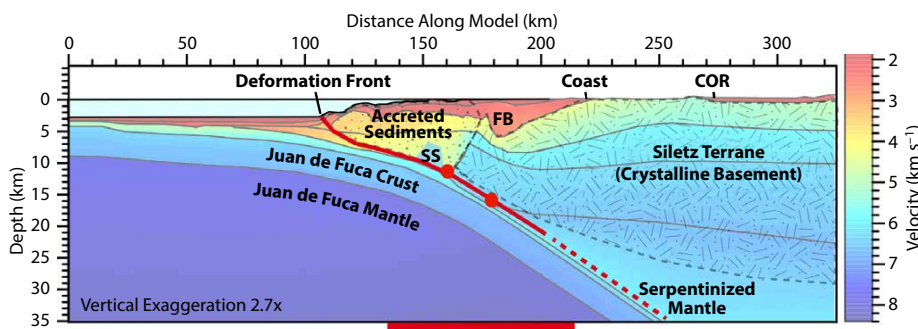


FIGURE 2. Interpreted cross section through the Cascadia subduction zone near latitude 44.65°N. The velocity model of Gerdom et al. (2000) is overlain by a geologic interpretation. The red line represents the plate boundary (dashed where the modeled plate boundary temperature is >450°C). Red dots indicate the projected positions of the two magnitude 4.7–4.8 earthquakes of 2004. The projected position of a subducted seamount (SS) based on magnetic anomaly data is also shown (Figure 3A). The basement rocks of the upper plate in this region are formed by mafic rocks of the Siletz terrane, anomalously thick oceanic crust that was accreted to North America ~50 million years ago and that is slowly moving northward and rotating relative to the core of North America, effectively acting as a microplate known as the Oregon Block (McCaffrey et al., 2007). Seaward of the Siletz terrane, the upper plate is composed of folded and faulted accreted sediments and slope sediments captured in basins formed through deformation and uplift of the margin. The seaward edge of the Siletz terrane is overlain by a forearc basin (FB). The red bar along the base of the figure indicates the region shown in Figure 4.

times is that the horizontal distance to the closest station should not exceed the depth. This condition is nearly always violated when land stations record off-shore events. Offshore seismic stations are required to locate earthquake epicenters accurately, obtain better estimates of source depth, and decrease the earthquake detection threshold. Although conventional OBSs (from which data are downloaded when the instrument is recovered) can be used to revise depth estimates post facto, real-time data are needed for routine earthquake monitoring.

Recent Seismicity on the Central Oregon Margin

Figure 3A shows a map of all earthquakes from January 1, 1989, through September 3, 2017, with magnitudes ≥ 3 between 43.5°N and 45.5°N and 126°W and 123°W. The data are from the US Geological Survey Advanced National Seismic System-Comprehensive Earthquake Catalog (ANSS-ComCat; see Figure 1 caption), which includes events reported by the PNSN and other regional

networks. While earthquakes are scattered throughout this region, most seismicity has occurred in clusters labeled N, S_A , and S_B . The largest event in these clusters was a magnitude 4.8 earthquake in cluster S_A in July 2004 and a magnitude 4.7 earthquake in cluster N in August 2004 (Tréhu et al., 2008). These two events were large enough to generate low-frequency energy within the noise notch (see below), permitting determination of the source mechanism and depth through moment tensor inversion of the waveforms recorded by regional seismic networks. From moment tensor inversion, with additional support from travel-time analysis of secondary seismic phases (pP, PmP, and SmS) observed on distant and regional seismic stations, Tréhu et al. (2008) concluded that these were low-angle thrust earthquakes that occurred on or near the plate boundary.

When smaller earthquakes in these clusters are relocated (Tréhu et al., 2015, and references therein), either by determining their depth relative to the two larger earthquakes or by including OBS

data when available, they define a surface dipping about 12° to the east (Figure 4), corresponding to the plate boundary identified in previous controlled source imaging experiments (Figure 2). This activity may result from grinding of a buried seamount against the seaward edge of crystalline basement (labeled “Siletz terrane” in Figure 2). Cluster S_B was first identified as being distinct from S_A when four nearly identical earthquakes with magnitudes of 2.8–3.4 occurred on January 25, 2013. The three clusters continue to produce earthquakes large enough to be detected by the onshore network at a rate of about six events per year.

In map view, earthquake locations obtained through these detailed studies are similar to those obtained through PNSN analyses, although the clusters are better defined. The earthquake depths and their relationship to the plate boundary structure, however, are significantly affected by the lack of offshore stations and by the simplified velocity models used in routine PNSN analysis (Figure 4).

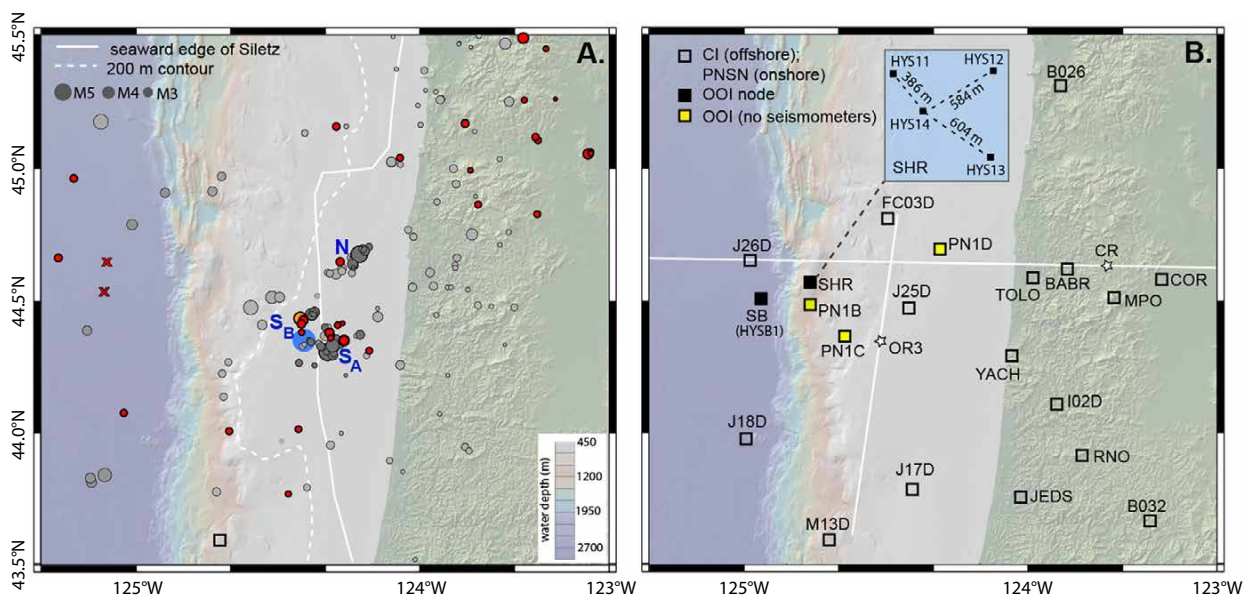


FIGURE 3. (A) Seismicity in the central Cascadia subduction zone. Dark gray circles mark earthquakes relocated as discussed by Tréhu et al. (2015); light gray circles are epicenters from the Pacific Northwest Seismic Network (PNSN) catalog prior to 2015 that have not been relocated; red dots denote earthquakes reported by PNSN from January 2015 through September 2017. Dot sizes are proportional to magnitude. N, S_A , and S_B indicate clusters of seismicity discussed in the text. The blue circle marks a subducted seamount inferred based on magnetic anomaly data (Tréhu et al., 2015). (B) Ocean Observatory Initiative (OOI) nodes and Cascadia Initiative (CI) and PNSN seismic stations used for this study. The inset shows the configuration of the four-station OOI array at Southern Hydrate Ridge (SHR); those labeled HYS11–13 are short period seismometers, and HYS14 is a broadband seismometer. Broadband seismometer HYSB1 is at node Slope Base (SB). White lines show the locations of two-dimensional velocity models discussed by Gerdorf et al. (2000); stars locate one-dimensional velocity models used in this study. Velocity models are shown in Supplementary Figure S5.

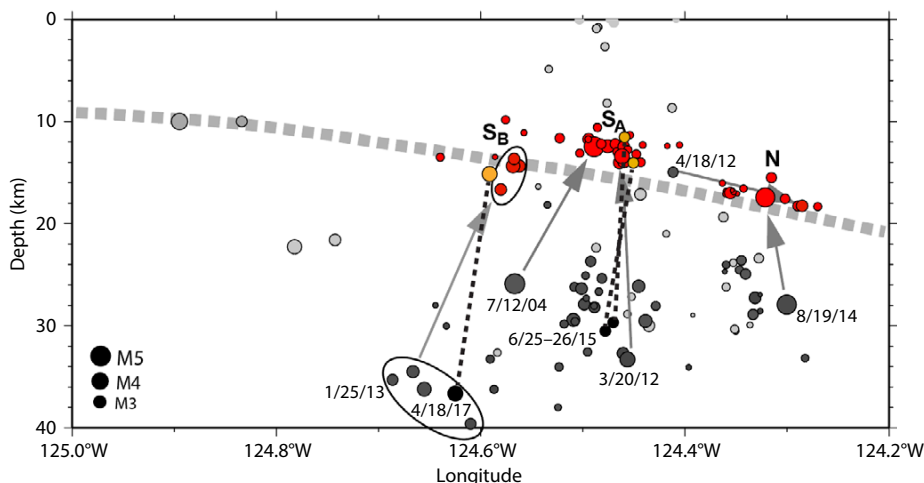


FIGURE 4. Cross section showing earthquake depths compared to the plate boundary in Figure 2. Circle radius is proportional to magnitude. Events in red were relocated by Tréhu et al. (2015); dark gray circles show PNSN locations for these events. Light gray circles are catalog events that were not relocated either because they were too small or they occurred prior to 2000 when there were too few stations (e.g., larger events west of 124.8°W). Relocations done for this study are in orange. Clusters labeled N, S_A , and S_B are discussed in the text and shown in map view in Figure 3A. Gray arrows (from Tréhu et al., 2015) and dashed lines (this study) illustrate relocated depths for selected events.

RESULTS OF NEW ANALYSES ENABLED BY THE OOI SEISMOMETERS

To examine the impact of including OOI stations in routine operations and the potential of augmenting the offshore array by instrumenting additional existing OOI nodes with seismometers, we compare OOI and OBS noise levels and look at three “case studies” of earthquakes occurring since 2014. Figure 3B shows the locations of OOI nodes, Cascadia Initiative OBSs, land seismic stations, and velocity models used in this study.

Noise Levels

Considerable effort has been devoted to understanding the characteristics of seismic noise in the ocean to improve recordings of teleseismic earthquakes on broadband OBSs (Webb, 1998). Broadband seismometers are best deployed in boreholes (Montagner et al., 1994; Collins et al., 2001), but where they are not available, shallow burial is preferred to emplacement on the seafloor because it ensures good ground coupling and shields the seismometer from ocean currents.

All seismic stations of the SB-SHR network are buried. The broadband stations

at SHR and SB were placed beneath the seafloor following an approach described by Romanowicz et al. (2003). A section of PVC pipe was inserted into the sediments to form a caisson, the sediments were evacuated from inside, the seismic sensor was enclosed in a spherical housing and placed at the bottom of the caisson so as not to touch the walls (online Supplementary Figure S1), and the caisson was covered with glass beads flush with the seafloor. The three short-period sensors at SHR are contained in narrow titanium cylinders that were buried by inserting them into a groove gouged by the arm of a remotely operated vehicle (Supplementary Figure S2); the groove was then filled with glass beads.

Figure 5A compares noise power spectra from the vertical channel of the two OOI broadband seismometers with those from a station located 20 km inland (BABR) and from three autonomous seafloor OBSs from the Cascadia Initiative experiment. From 0.1 Hz to 3 Hz, the noise spectra are dominated by microseism peaks, which have higher amplitudes at the seafloor stations compared to the land station because they are generated by nonlinear interactions of ocean

waves (Webb, 1998). At frequencies immediately below the microseism peak, there is a low-noise notch on all stations except for J25C. This is the signal band used for inversion of waveform data to obtain moment tensor estimates. At the seafloor stations, the noise level increases at lower frequencies because the pressure perturbations from infragravity waves (long-wavelength ocean waves) reach the seafloor. In shallow water, the infragravity wave noise extends to higher frequencies and impinges on, and in the case of station J25C eliminates, the low-noise notch. Processing techniques can remove this noise from the vertical channel using data from the horizontal channels or a coincident seafloor pressure sensor (e.g., Crawford and Webb, 2000).

From 3 Hz to 20 Hz, the noise levels onshore and at three of the five seafloor stations, including the two OOI stations, are remarkably similar (Figure 5A). This signal band is needed to pick travel times of P- and S-waves from local earthquakes. Figure 5B shows noise levels at 5 Hz recorded by Cascadia Initiative and OOI seismometers as a function of water depth. For the Cascadia Initiative OBSs, the noise levels are quite scattered, but increase markedly at shallower depths. This likely reflects poor coupling of the sensors to the seafloor, noise induced by components of the OBS package in the presence of strong ocean currents, and frequent impulsive signals due to biological activity, which can number in the thousands per day at water depths <500 m (Williams et al., 2010). Burying the seismometers, as was done for the OOI instruments, shields the sensors from currents and fauna, leading to lower noise levels at higher frequencies.

Modeling the Impact of Offshore Stations on Detection Levels Using Site-Specific Noise Characteristics

Figure 6 shows the results of applying the method of McNamara et al. (2016) to develop a series of magnitude detection threshold maps for different seismic

network configurations by combining site-specific spectral noise characteristics with simple earthquake source and wave propagation models. If the ground motion at a station from a model earthquake exceeds the noise model at any frequency, we infer that the station detects the earthquake. Detections at four stations result in a network detection and hence a locatable earthquake. To investigate potential improvements in detection capability that might result from adding offshore stations to the current onshore seismic network, we used modal noise profiles derived from OOI and Cascadia Initiative stations, which represent the most likely noise levels at hypothetical sites. We also use modal noise values for PNSN onshore stations.

These maps represent a best-case scenario because a signal just above noise does not guarantee an automatic detection; in practice, signal must exceed noise by some (difficult to quantify) amount. However, the method is consistent and objective, and thus useful for comparing network detection performance. Figure 6A shows the detection threshold from the onshore seismometers and current OOI SB-SHR and Axial Seamount (see Wilcock et al., 2018, in this issue) networks using noise profiles computed for a randomly selected month. The detection threshold is very low onshore and shows how clusters of

stations can further reduce the detection threshold locally in regions of particular interest. Offshore, the detection threshold increases smoothly with increasing distance from the network, with locally lower-magnitude detection thresholds in

the immediate vicinity of the OOI networks. Figure 6B shows how an ambitious offshore network of buried seismometers would impact the detection threshold, assuming noise levels characteristic of OOI sites and a station distribution

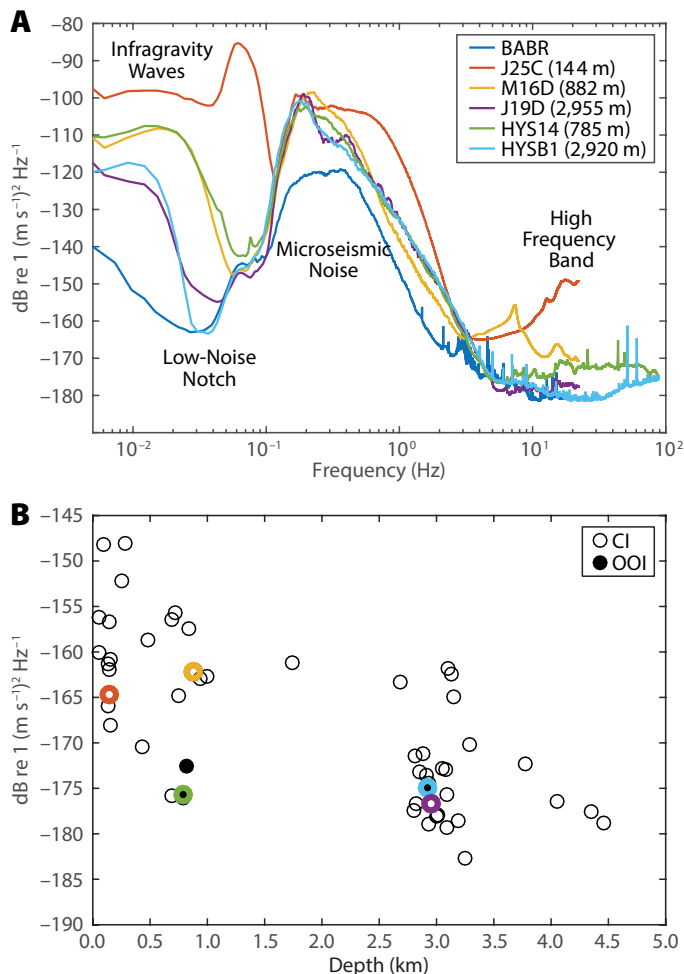


FIGURE 5. (A) Velocity power spectra for background noise on the vertical broadband channels of selected PNSN (BABR), CI (J25C, J19D, M16D), and OOI (HYS14, HYSB1) sites, with water depths indicated. Spectra were calculated with one-hour data windows over one year; median values are plotted. (B) Median noise levels at 5 Hz as a function of instrument depth for all Cascadia Initiative OBSs deployed in 2014–2015 and for the OOI stations. Color corresponds to sites shown in (A).

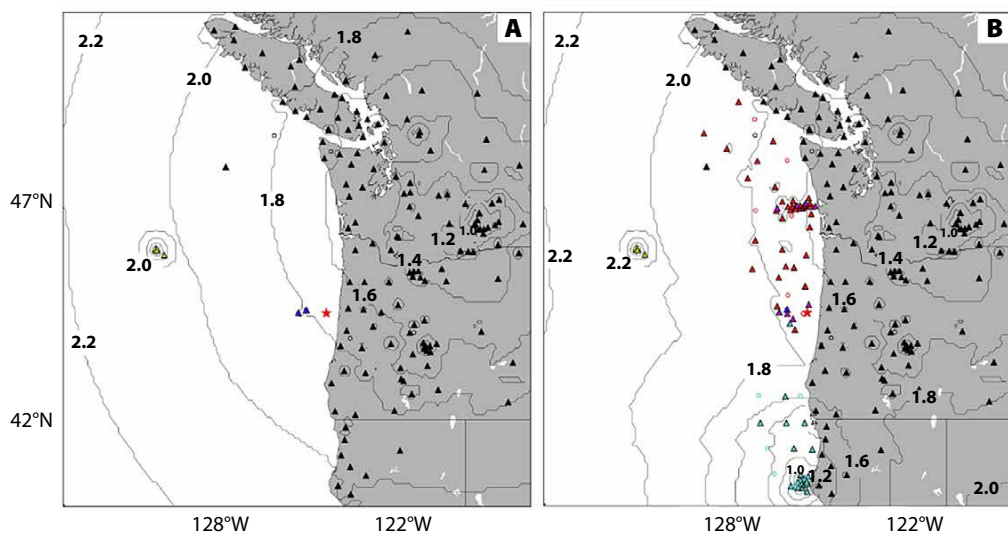


FIGURE 6. (A) Magnitude detection threshold in Cascadia using existing onshore stations and offshore cabled seismometers (OOI and NEPTUNE networks). Contours show the minimum magnitude that would be detected by at least four stations (see text for details). Black triangles are onshore seismic stations. Circles are stations that did not contribute to any of the four detections used to determine the threshold. The red star marks the approximate location of interplate earthquakes (Figure 3A). (B) As for (A), but with stations added at additional existing OOI nodes (violet triangles) and at Cascadia Initiative OBS locations along the margin in 2012 (red triangles) and 2013 (cyan triangles).

similar to the Cascadia Initiative network along the Cascadia subduction margin.

This exercise indicates that improvement in the detection threshold for offshore earthquakes along the continental margin is decreased, although a significant decrease in the magnitude detection threshold would require a large investment. However, it is important to note that this analysis considered only detectability. The impact of offshore stations on the resolution of earthquake source depth, a parameter that is important for understanding the tectonic and hazard implications of seismicity, is discussed in the next section. It also does not include the impact of T-phases on detections, as discussed in the penultimate section.

The Importance of Close Stations for Determining Earthquake Depth: Case Study of the June 25–26, 2015, Earthquakes

The PNSN catalog includes two magnitude 2.5 earthquakes on June 25 and 26 with locations in cluster S_A and nominal source depths of about 30 km. To relocate these events, we picked P and S arrival times from seismic stations within about 120 km of the epicenter, including the OOI stations, Cascadia Initiative OBSs,

and onshore stations. Figure 7A compares data from broadband OOI station HYS14 in the SHR network to data from onshore broadband station BABR. Both stations were located about 60 km from the earthquake and show clear, impulsive P- and S-wave arrivals, and the signal-to-noise ratio is similar in the 1–20 Hz frequency band. Although not shown here, signal-to-noise ratios are also similar at SB (broadband station HYSB1) and on short-period stations HYS11–13 in the SHR network.

Figure 7B compares the P-waves recorded on HYSB1 and HYS14 to P-waves recorded on several Cascadia Initiative OBSs, including J25D, which was the station closest to the epicenter. Although P and S first arrivals are impulsive on J25D, the signal-to-noise ratio at distances >50 km is quite variable. While this may be due in part to the radiation pattern of the earthquake, it may also be due to effects of soil-structure interaction, bottom current activity, and other noise sources that affect OBSs more strongly than the buried OOI seismometers, as discussed in the previous section. Note that although FC03D is closer to the source than HYS14, and J17D is closer than HYSB1, the noise levels are lower at

the OOI site than at the Cascadia Initiative site for both of these station pairs.

Earthquakes were located in one-dimensional velocity models. All stations were normalized to sea level by applying station corrections based on the velocity of the uppermost layer in the model (2.5 km s^{-1}) to correct for different station elevations. This results in station corrections that range from -1.23 s for OBS station J10D to 1.15 s for onshore station B032 and is equivalent to removing the Coast Range and filling the ocean with sediment.

Results for the event on June 25, 2015, at 20:25 based on two different one-dimensional P-wave velocity models were compared. See Supplementary Figure S3 for details. The first model was extracted from a two-dimensional velocity model of the continental margin derived from controlled-source imaging at the position marked OR3 in Figure 3B. The second model is appropriate for the Coast Range (CR on Figure 3B) and is similar to the model used by PNSN to locate earthquakes in this region. For both models, we assumed a ratio of P-wave to S-wave velocity of 1.77, which is a typical value for crustal rocks, although it is low for marine sediments. To test the sensitivity

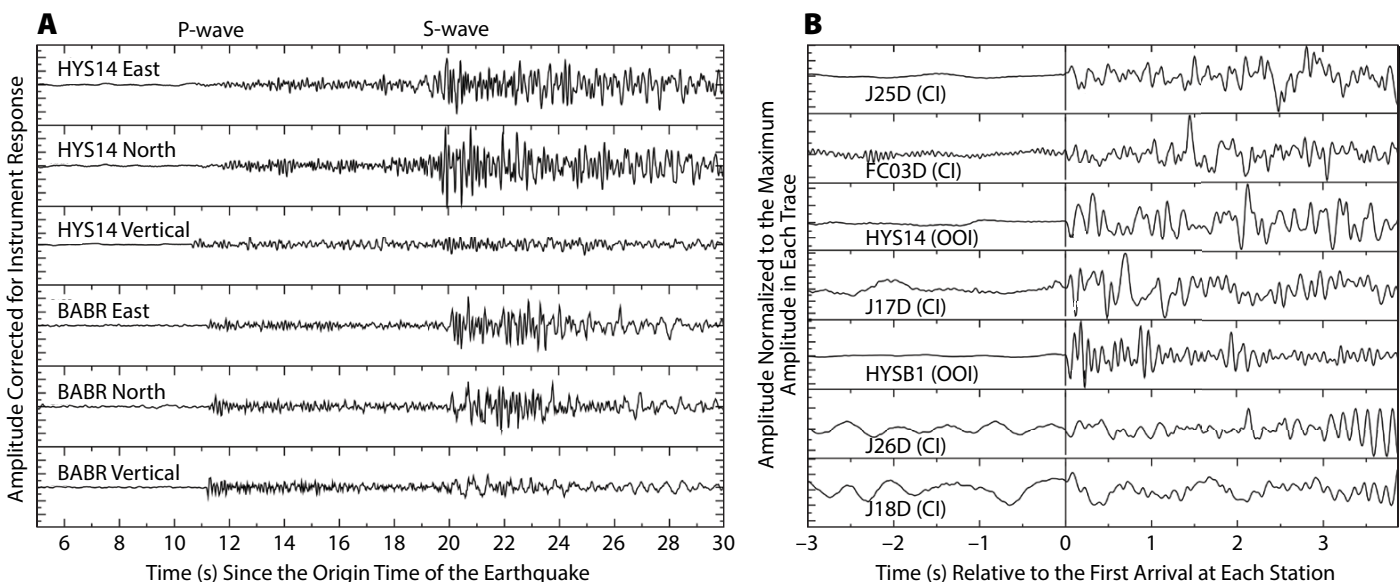


FIGURE 7. Waveforms for the July 25, 2016, earthquake in cluster S_A . Data have been high-pass filtered at 1 Hz to remove microseismic noise. (A) Comparison of three-component broadband waveforms for stations HYS14 and BABR. (B) P-waveforms recorded on the vertical component of OOI and OBS broadband seismometers ordered with source-receiver distance (17–93 km) increasing from top to bottom. Waveforms are aligned on the P-arrival pick.

of the solution to source depth, we determined the best-fitting source latitude, longitude, and origin time for a series of fixed source depths and compared the misfit for the different velocity models and various subsets of data.

The effect of velocity model uncertainty on the source latitude and longitude is small. All solutions are within about 2 km of each other (and of the epicenter reported by PNSN), which is consistent with the nominal horizontal uncertainties. The best-fit source depth, however, depends strongly on the velocity model, with model OR3 leading to shallow source depths (<15 km) and model CR leading to deeper depths (>30 km). Moreover, the misfit for OBS station J25D, located ~17 km from the epicenter, is small only for depths of 8–13 km independent of the velocity model used. Addition of seismometers to existing OOI nodes that do not currently have them (Figure 3B) would be of great benefit for improving the depth resolution when locating earthquakes along this anomalously active segment of the margin.

A Test of the Broadband Data from the OOI Seismometers: The April 15, 2017, Earthquake

The magnitude 3.8 event in subcluster S_B on April 15, 2017, was large enough to generate long-period waves suitable for moment tensor inversion. Results of that analysis are shown in Figure 8. Data at periods of 12–20 s and velocity model OR3 were used for the inversion. Stable moment tensor inversions near coasts, where the microseismic noise is strong, require using seismic waves in the frequency band of the low-noise notch (Figure 5A), which are not excited strongly enough to rise above background noise levels for earthquakes with magnitudes less than about 3.2.

Figure 8A shows several examples of the data and the waveforms predicted for the best-fitting solution, which has a depth of 12 km, and for a solution with a depth of 36 km, which is close to the depth in the

PNSN catalog (38 km). Figure 8B shows the focal mechanism (type of faulting in the source region) of the best-fit solution along with azimuthal data coverage. Figure 8C shows the residual for the inversion as a function of depth and the focal mechanism for the solution at each depth. If the OOI data are not included, the misfit decreases by ~0.05 s at each depth and the focal mechanism and source depth are not significantly different. The increased misfit when OOI data are included is likely due to higher noise levels on the horizontal components of the OOI broadband seismometers. Although inclusion of the OOI data did not significantly affect the moment tensor solution in this case, this exercise demonstrated that the

OOI broadband data are useful for low-frequency waveform modeling.

We conclude that this earthquake was a thrust event near the plate boundary. The fault dip appears to be ~45° on either an east-dipping or west-dipping plane. The focal mechanism is similar to that of a magnitude 3.8 earthquake in cluster S_A on March 20, 2012 (Tréhu et al., 2015), and somewhat different from that of the two larger earthquakes in 2004 (Tréhu et al., 2008). These results suggest a scenario in which the subducted seamount is acting as an asperity (lock on the fault) that is generating earthquakes around its edges or in the lower crust of the upper plate (Wang and Bilek, 2011). The implications of these observations for estimates of

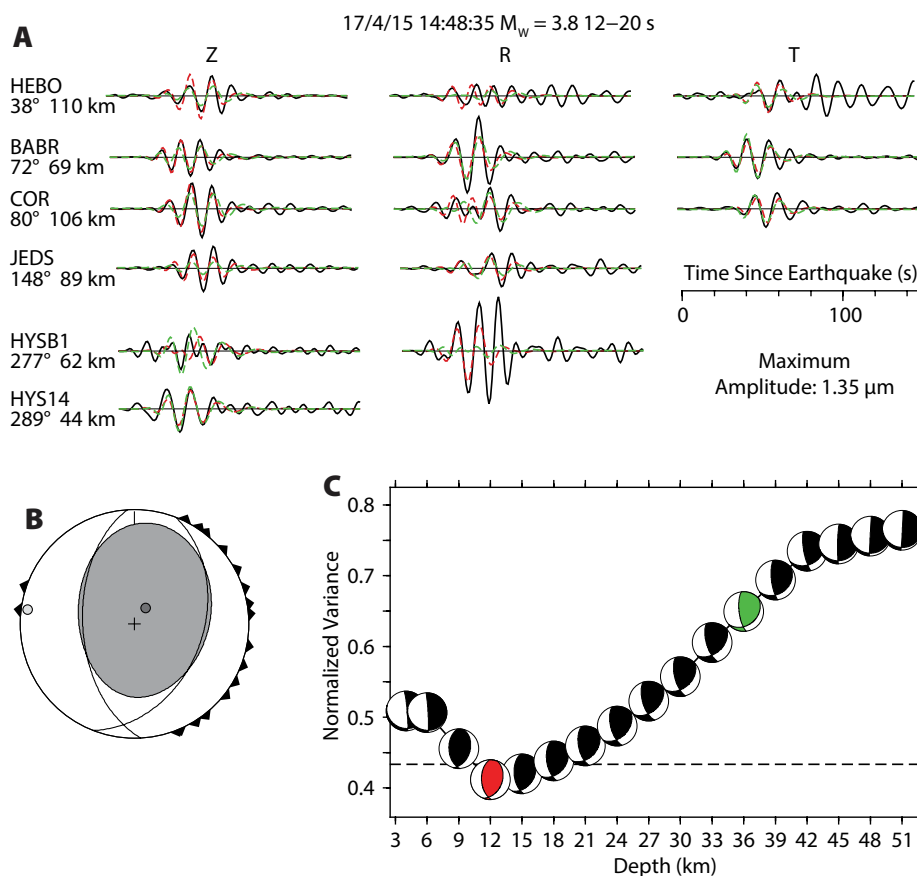


FIGURE 8. Moment tensor inversion for the April 15, 2017, magnitude 3.8 earthquake. (A) Examples of observed (black lines) long period waveforms (12–20 s period) compared to waveforms predicted for the preferred solution at 12 km depth (red dashed lines) and at 36 km depth (green dashed lines). In addition to the two OOI stations, 15 onshore broadband stations were used to obtain this solution. (B) Best-fit source mechanism, including a minor non-double couple component that is likely due to noise, has a nearly horizontal compression axis oriented at 275° and indicates thrust faulting on a plane dipping ~45°. Triangles on the outside of the focal sphere indicate azimuth of stations used. (C) Normalized variance and corresponding best-fit double couple solution as a function of assumed source depth. Red and green mechanism diagrams correspond to red and green seismograms in (A).

Cascadia earthquake hazard are unclear, and continued monitoring of this region with improved capability to resolve the source depth and mechanism is needed.

Events Detected by the OOI Network That Are Not Reported by Onshore Networks

We visually scanned all data collected from January 1 to August 15, 2017, at stations HYS11-14 and HYSB1 to determine if any local signals were recorded across the SB-SHR network that were not reported by the PNSN. Visual scans are a preliminary step toward identification of potential “templates” for automated searching of the data for additional earthquakes (Morton and Bilek, 2015) and other seismic signals. The dense network of stations at the summit of SHR (inset in Figure 3B) was designed, in part, to detect possible seismic tremor or low-frequency earthquakes generated by pulses of fluid motion associated with known methane vents.

We detected two small events in 2017, one on January 4 and one on April 18, that were clearly recorded across the OOI array

and were not reported by the land network because they were not clearly recorded on enough stations to trigger a detection (Supplementary Figure S4). These events have been tentatively located ~50 km northwest of station HYSB1 (Figure 3B) and may represent earthquakes in the subducting plate as it approaches the deformation front. A number of earthquakes in this general region have been reported in the past, including a magnitude 5.8 event in 1973 (Spence, 1989). The OOI seismic stations at SB, SHR, and Axial Seamount have the potential to decrease the detection threshold and improve the accuracy of earthquake locations within this part of the Juan de Fuca Plate, improving knowledge of the tectonics of this region and the relationship between intraplate deformation and subduction.

Another type of event recorded on the OOI SB-SHR network, but not onshore, is energy from submarine earthquakes that couples into the SOFAR channel and produces a packet of energy that follows the P (primary) and S (secondary) waves. These are generally known as T (tertiary) phase. Figure 9 shows aftershocks

associated with a swarm of earthquakes (including two events with magnitudes of 5.8 and 5.9) on the Blanco Transform Fault on June 1, 2015. In the hour following the magnitude 5.8 event, the ANSS ComCat catalog includes six earthquakes (the smallest of magnitude 3.9). During that same time period, T-phases from more than 20 smaller amplitude events were detected on the OOI network. Future work includes determination of magnitudes based on T-phase amplitudes (e.g., Dziak, 2001) to increase the magnitude range available for detailed analysis of swarm characteristics, which can provide clues to in situ stress state and earthquake dynamics.

CONCLUSIONS

The OOI seismometers contribute significantly to the ability of the regional seismic network in the Pacific Northwest to monitor the temporal evolution of seismic activity. Offshore sensors are critical for determining earthquake source depths, which are important for understanding Cascadia interplate dynamics. The OOI data are available immediately and can be incorporated into routine locating procedures, unlike data from traditional ocean bottom seismometers. Moreover, data quality is comparable to that recorded on coastal stations, unlike data from ocean bottom seismometers, for which local effects of seafloor currents, biological activity, and OBS-sediment coupling differences due to different package designs can lead to considerable variability in the effective signal-to-noise ratio. Although the magnitude detection threshold based only on P- and S-waves is significantly decreased primarily in the immediate vicinity of the stations, analysis of T-phases, recorded only on offshore stations, promises to decrease the detection levels for earthquakes occurring throughout the region. Expansion of the seismic network to the three active nodes on the central Cascadia margin that are not presently equipped with seismometers would improve depth resolution for events along a segment of the margin that has been

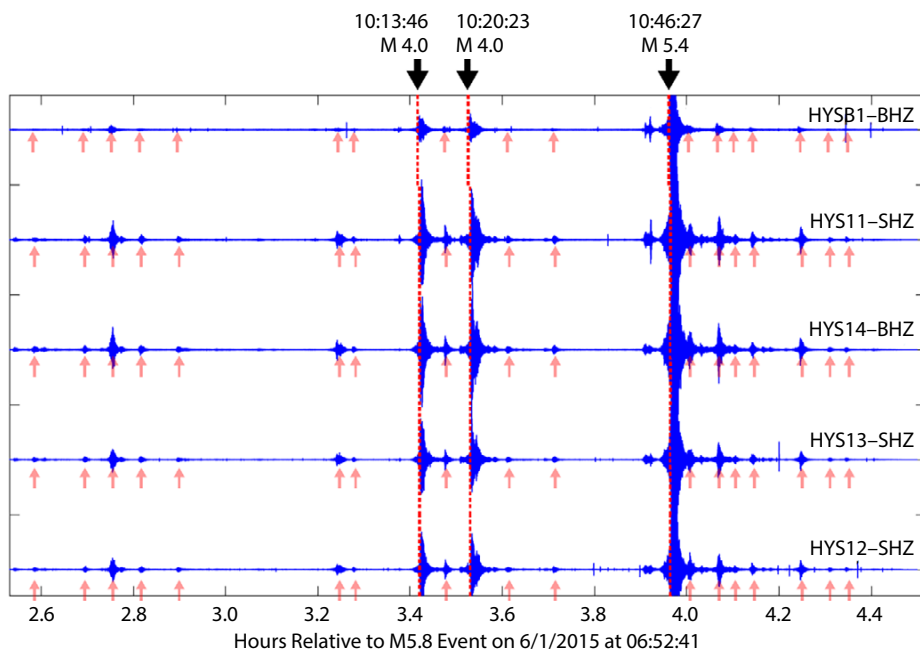



FIGURE 9. T-phases recorded on the vertical component of the OOI SB-SHR network from a swarm of earthquakes on the Blanco Transform Fault that occurred on June 1, 2015. The red dashed lines show T-phases from earthquakes in the ANSS Comprehensive Earthquake Catalog. Time and magnitude are indicated. The pink arrows show T-phases interpreted to be from additional, smaller earthquakes.

anomalously seismically active for the past several decades when compared with segments to the north and south. Significant expansion of the cabled network would be necessary to provide equivalent capability along the entire margin. 

SUPPLEMENTARY MATERIALS

Supplementary Figures S1–S5 are available online at <https://doi.org/10.5670/oceanog.2018.116>.

REFERENCES

- Atwater, B.F., S. Musumi-Rokkaku, K. Satake, Y. Tsuji, K. Ueda, and D.K. Yamaguchi. 2015. *The Orphan Tsunami of 1700: Japanese Clues to a Parent Earthquake in North America*, 2nd ed. US Geological Survey Professional Paper 1707, Seattle, University of Washington Press, 135 pp, <https://pubs.er.usgs.gov/publication/pp1707>.
- Bouchon, M., V. Durand, D. Marsan, H. Karabulut, and J. Schmittbuhl. 2013. The long precursory phase of most large interplate earthquakes. *Nature Geoscience* 6:299–302, <https://doi.org/10.1038/ngeo1770>.
- Burgmann, R. 2014. Warning signs of the Iquique earthquake. *Nature* 512:258–259, <https://doi.org/10.1038/nature13655>.
- Collins, J.A., F.L. Vernon, J.A. Orcutt, R.A. Stephen, K.R. Peal, F.B. Wooding, F.N. Speiss, and J.A. Hilderbrand. 2001. Broadband seismology in the oceans: Lessons from the Ocean Seismic Network Pilot Experiment. *Geophysical Research Letters* 28(1):49–52, <https://doi.org/10.1029/2000GL011638>.
- Crawford, W.C., and S.C. Webb. 2000. Identifying and removing tilt noise from low-frequency (<0.1 Hz) seafloor vertical seismic data. *Bulletin of the Seismological Society of America* 90:952–963, <https://doi.org/10.1785/0119990121>.
- Cozzens, B.D., and G.A. Spinelli. 2012. A wider seismogenic zone at Cascadia due to fluid circulation in subducting oceanic crust. *Geology* 40(10):899–902, <https://doi.org/10.1130/G330191>.
- deMets, C., R.G. Gordon, and D.F. Argus. 2010. Geologically current plate motions. *Geophysical Journal International* 181(1):1–80, <https://doi.org/10.1111/j.1365-246X.2009.04491.x>.
- Dziak, R. 2001. Empirical relationship of T-wave energy and fault parameters of Northeast Pacific ocean earthquakes. *Geophysical Research Letters* 28:2,537–2,540, <https://doi.org/10.1029/2001GL012939>.
- Gerdorf, M., A.M. Tréhu, E.R. Flueh, and D. Klaeschen. 2000. The continental margin off Oregon from seismic investigations. *Tectonophysics* 329:79–97, [https://doi.org/10.1016/S0040-1951\(00\)00190-6](https://doi.org/10.1016/S0040-1951(00)00190-6).
- Goldfinger, C., C.H. Nelson, A. Morey, J.E. Johnson, J. Gutierrez-Pastor, A.T. Eriksson, E. Karabanov, J. Patton, E. Gracia, R. Enkin, and others. 2012. *Turbidite Event History: Methods and Implications for Holocene Paleoseismicity of the Cascadia Subduction Zone*. US Geological Survey Professional Paper 1661-F, Reston, VA, 332 pp, https://pubs.usgs.gov/pp/pp1661f/pp1661f_text.pdf.
- Hyndman, R.D. 2013. Dwindling landward limit of Cascadia great earthquake rupture. *Journal of Geophysical Research* 118(10):5,530–5,549, <https://doi.org/10.1002/jgrb.50390>.
- Hyndman, R., and K. Wang. 1993. Thermal constraints on the zone of major thrust earthquake failure: The Cascadia subduction zone. *Journal of Geophysical Research* 98(B2):2,039–2,060, <https://doi.org/10.1029/92JB02279>.
- Ito, Y., R. Hino, M. Kido, H. Fujimoto, Y. Osada, D. Inazu, Y. Ohta, T. Ilinuma, M. Ohzono, S. Miura, and others. 2013. Episodic slow slip events in the Japan subduction zone before the 2011 Tohoku-Oki earthquake. *Tectonophysics* 600:14–26, <https://doi.org/10.1016/j.tecto.2012.08.022>.
- McCaffrey, R., A.I. Qamar, R.W. King, R. Wells, G. Khazaradze, C.A. Williams, C.W. Stevens, J.J. Vollick, and P.C. Zwick. 2007. Fault locking, block rotation and crustal deformation in the Pacific Northwest. *Geophysical Journal International* 169(3):1,315–1,340, <https://doi.org/10.1111/j.1365-246X.2007.03371.x>.
- McNamara, D.E., C. von Hillebrandt-Andrade, J.-M. Saurel, V.R. Huerfano, and L. Lynch. 2016. Quantifying 10 years of improved earthquake-monitoring performance in the Caribbean region. *Seismological Research Letters* 87:26–36, <https://doi.org/10.1785/0220150095>.
- Montagner, J.-P., J.-F.O. Karczewski, B. Romanowicz, S. Bouaricha, P. Lognonné, G. Roulit, E.O. Stutzmann, J.-L. Thriot, J. Brion, B. Dole, and others. 1994. The French Pilot Experiment OFM-SISMOBS: First scientific results on noise level and event detection (1994). *Physics of the Earth and Planetary Interiors* 84(1):321–336, [https://doi.org/10.1016/0031-9201\(94\)90050-7](https://doi.org/10.1016/0031-9201(94)90050-7).
- Morton, E.A., and S.L. Bilek. 2015. Preliminary event detection of earthquakes using the Cascadia Initiative data. *Seismological Research Letters* 86(5):1,270–1,277, <https://doi.org/10.1785/0220150098>.
- Rogers, G., and H. Dragert. 2003. Episodic tremor and slip on the Cascadia subduction zone: The chatter of silent slip. *Science* 300:1,942–1,943, <https://doi.org/10.1126/science.1084783>.
- Romanowicz, B., D. Stakes, R. Uhrhammer, P. McGill, D. Neuhauser, T. Ramirez, and D. Dolenc. 2003. The MOBB experiment: A prototype permanent off-shore ocean bottom broadband station. *Eos, Transactions American Geophysical Union* 84(34):325–332, <https://doi.org/10.1029/2003EO340002>.
- Spence, W. 1989. Stress origins and earthquake potentials in Cascadia. *Journal of Geophysical Research* 94(B3):3,076–3,088, <https://doi.org/10.1029/JB094iB03p03076>.
- Toomey, D.R., R.M. Allen, A.H. Barclay, S.W. Bell, P.D. Bromirski, R.L. Carlson, X. Chen, J.A. Collins, R.P. Dziak, B. Evers, and others. 2014. The Cascadia Initiative: A sea change in seismological studies of subduction zones. *Oceanography* 27(2):138–150, <https://doi.org/10.5670/oceanog.2014.49>.
- Tréhu, A.M. 2016. Source parameter scaling and the Cascadia paleoseismic record. *Bulletin of the Seismological Society of America* 106:904–911, <https://doi.org/10.1785/0120150272>.
- Tréhu, A.M., J. Braunmiller, and E. Davis. 2015. Seismicity of the central Cascadia continental margin near 44.5°N: A decadal view. *Seismological Research Letters* 86:819–829, <https://doi.org/10.1785/0220140207>.
- Tréhu, A.M., J. Braunmiller, and J.L. Nabelek. 2008. Probable low-angle thrust earthquakes on the Juan de Fuca-North America plate boundary. *Geology* 36:127–130, <https://doi.org/10.1130/G24145A.1>.
- Wang, K., and S.L. Bilek. 2011. Do subducting seamounts generate or stop large earthquakes? *Geology* 39:819–822, <https://doi.org/10.1130/G31856.1>.
- Wang, K., and A.M. Tréhu. 2016. Invited review paper: Some outstanding issues in the study of great megathrust earthquakes—The Cascadia example. *Geodynamics* 98:1–18, <https://doi.org/10.1016/j.jog.2016.03.010>.
- Webb, S.C. 1998. Broadband seismology and noise under the ocean. *Reviews of Geophysics* 36(1):105–142, <https://doi.org/10.1029/97RG02287>.
- Wilcock, W.S.D., R.P. Dziak, M. Tolstoy, W.W. Chadwick Jr., S.L. Nooner, D.R. Bohnenstiehl, J. Caplan-Auerbach, F. Waldhauser, A.F. Arnulf, C. Baillard, and others. 2018. The recent volcanic history of Axial Seamount: Geophysical insights into past eruption dynamics with an eye toward enhanced observations of future eruptions. *Oceanography* 31(1):114–123, <https://doi.org/10.5670/oceanog.2018.117>.
- Williams, M.C., A.M. Tréhu, and J. Braunmiller. 2010. Local earthquake detection in marine environments using seismic signal parameters. *Eos, Transactions American Geophysical Union* 91, Abstract S53A-1965.

ACKNOWLEDGMENTS

Support for this work was provided by the US National Science Foundation (NSF) through grants to Oregon State University. NSF supports the OOI seismic network through a contract with the University of Washington. Support was also provided by the US Geological Survey through its support of the Pacific Northwest Seismic Network. The University of Washington also acknowledges support from the Gordon and Betty Moore Foundation. Data from the OOI, Cascadia Initiative, and PNSN stations used in this study are freely available from the IRIS Data Management Center (<https://ds.iris.edu/ds/nodes/dmc/>).

AUTHORS

Anne M. Tréhu (trehu@coas.oregonstate.edu) is Professor, College of Earth, Ocean and Atmospheric Sciences, Oregon State University, Corvallis, OR, USA. William S.D. Wilcock is Jerome M. Paros Endowed Chair in Sensor Networks, Rose Hilmo is a graduate student, Paul Bodin is Research Professor, Jon Connolly is Software Engineer, and Emily C. Roland is Assistant Professor, all at the College of the Environment, University of Washington, Seattle, WA, USA. Jochen Braunmiller is Research Assistant Professor, School of Geosciences, University of South Florida, Tampa, FL, USA.

ARTICLE CITATION

Tréhu, A.M., W.S.D. Wilcock, R. Hilmo, P. Bodin, J. Connolly, E.C. Roland, and J. Braunmiller. 2018. The role of the Ocean Observatories Initiative in monitoring the offshore earthquake activity of the Cascadia subduction zone. *Oceanography* 31(1):104–113, <https://doi.org/10.5670/oceanog.2018.116>.